2

Steady flows bounded by plane boundaries

2.1 Plane Couette–Poiseuille flow

We begin this discussion with a consideration of the simplest of flows, namely that between parallel plane boundaries under the action of a pressure gradient parallel to the boundaries in, say, the x-direction with one boundary sliding in that direction. It suits our purpose to generalise the situation by allowing fluid to be injected with uniform constant velocity at one boundary, and similarly removed at the other. Such flows, driven solely by a pressure gradient, are associated with Poiseuille (1840) who was concerned with the flow in tubes as discussed in the next chapter. Flows driven by the sliding or 'scraping' motion of the boundary were considered by Couette (1890).

With x measured in the flow direction, and y perpendicular to the plane boundaries, assumed to be at $y = 0, h$, we have $\mathbf{v} = (u, v, 0)$ and we assume that $u = u(y)$, $v = v(y)$. That is, we assume the flow to be fully developed, and so independent of any entry conditions to the channel. The Navier–Stokes equations, then, are to be solved subject to the conditions

$$\begin{aligned} u &= 0, \quad v = V \quad \text{at} \quad y = 0, \\ u &= U, \quad v = V \quad \text{at} \quad y = h. \end{aligned} \tag{2.1}$$

From (1.12) we see at once that $\partial v/\partial y = 0$, and hence $v \equiv V$. In the absence of any body force equation (1.10) shows that $\partial p/\partial y = 0$ so that $p = p(x)$, and the equation we must solve, namely (1.9), reduces to

$$V\frac{\partial u}{\partial y} = -\frac{1}{\rho}\frac{\partial p}{\partial x} + \nu\frac{\partial^2 u}{\partial y^2}. \tag{2.2}$$

From the assumptions we have made, it is clear from (2.2) that the pressure gradient is a constant, and we set $\partial p/\partial x = -P$. The solution, then, of (2.2)

subject to (2.1) is

$$u(y) = \frac{P}{\rho V} y + U\left(1 - \frac{Ph}{\rho U V}\right)\left(1 - \mathrm{e}^{Vy/\nu}\right) / \left(1 - \mathrm{e}^{R}\right), \tag{2.3}$$

where $R = Vh/\nu$ is a Reynolds number. In the limit as $V \to 0$, when the boundaries are impermeable, we recover the classical Couette–Poiseuille solution

$$u(y) = U\frac{y}{h} + \frac{1}{2}\frac{Ph^2}{\mu}\left\{\frac{y}{h} - \left(\frac{y}{h}\right)^2\right\}. \tag{2.4}$$

If we define Q as the mass flux along the channel per unit depth, then we have

$$Q = \int_0^h \rho u \, \mathrm{d}y = \frac{1}{2}\rho U h\left(1 + \frac{Ph^2}{6\mu U}\right). \tag{2.5}$$

For $U < 0$ there is a region close to $y = h$ in which the flow is reversed in direction, whilst for U sufficiently large and negative, such that $U < -Ph^2/6\mu$, there is a net mass flux in the negative x-direction.

We note that if $U = Ph^2/2\mu$ then $\partial u/\partial y = 0$ at $y = h$, which implies that the boundary $y = h$ behaves as a free surface. Indeed, if we let $P = \rho g \sin\alpha$, where g is the acceleration due to gravity, we have, in that case,

$$u(y) = \frac{\rho g h^2 \sin\alpha}{2\mu}\left\{2\frac{y}{h} - \left(\frac{y}{h}\right)^2\right\}, \tag{2.6}$$

which represents the fully developed flow of a film of viscous fluid, thickness h, down a plane inclined at angle α to the horizontal in the presence of the body force per unit mass $\mathbf{F} = (-g\sin\alpha, -g\cos\alpha, 0)$. The free-surface speed is $\rho g h^2 \sin\alpha/2\mu$, and $Q = \rho g h^3 \sin\alpha/3\nu$. Sample velocity profiles are shown in figure 2.1.

Returning next to the case of permeable walls, for which $v \equiv V$ and u is as in equation (2.3), we have for the limiting situation $V \gg \nu/h$, $Ph/\rho U$, the velocity $u(y) \approx U\exp\{V(y-h)/\nu\}$ so that u is essentially zero except close to $y = h$, specifically where $h - y = O(\nu/V)$ where u increases rapidly to the boundary velocity U. Conversely, if we reverse the injection velocity, and write $V = -\overline{V}$, then for $\overline{V} \gg \nu/h$, $Ph/\rho U$ we have $u(y) \approx U\{1 - \exp(-\overline{V}y/\nu)\} \approx U$ except for $y = O(\nu/\overline{V})$ where again a rapid transition takes place, in a thin 'boundary layer', to enable satisfaction of the no-slip condition. In this latter case fluid particles emerge into the fluid, at $y = h$, with momentum $U\mathbf{i} - \overline{V}\mathbf{j}$ per unit mass. This remains unchanged, by either pressure or viscous forces, until viscous stresses destroy the x-component close to $y = 0$. The boundary vorticity $\zeta_w = -U\overline{V}/\nu$, and as we have seen this penetrates, by diffusion, a distance only $O(\nu/\overline{V})$ from the boundary, restrained as it is by convection towards it.

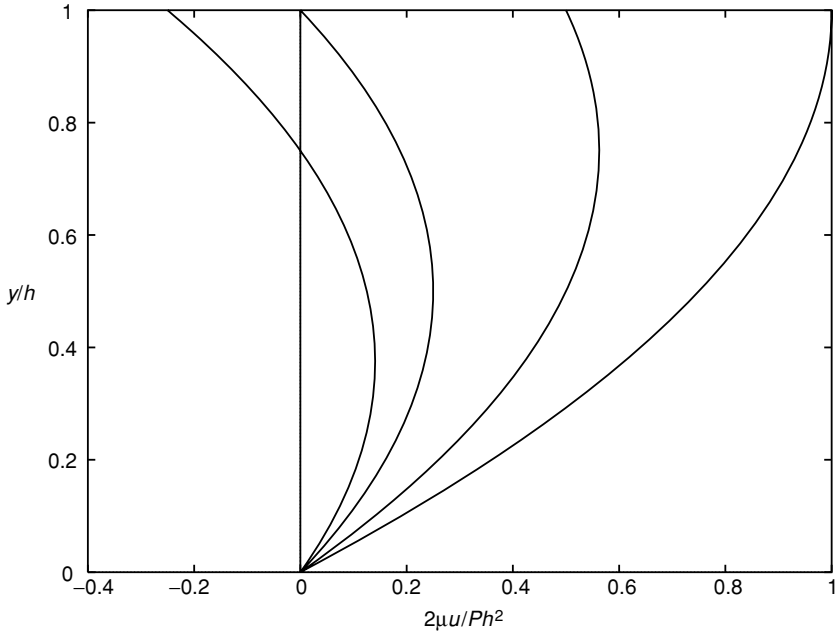

Figure 2.1 Velocity profiles in Couette–Poiseuille flow from equation (2.4) with, from the left, $2\mu U/Ph^2 = -1/4$, 0, 1/2, 1 respectively.

Kolmogorov (see Meshalkin and Sinai 1961) discussed a special class of forced flows in his seminar in Moscow on selected problems in analysis. These are the class of flows for which $\mathbf{F} = \gamma \sin(\pi y/h)\mathbf{i}$, $-h \le y \le h$ so that $p =$ constant, $u = (\gamma h^2/\pi^2 \nu)\sin(\pi y/h)$ and $Q = 0$. Whilst the forcing and flow are artificial, the flow has served as a prototype to model spatially periodic flows, such as waves, and their instability.

Several solutions for flow in channels of finite cross-section, S, bounded by plane boundaries, for which $\mathbf{v} = \{u(y, z), 0, 0\}$, are available. For such situations we have, from equations (1.9) to (1.12) and in the absence of body forces

$$\frac{\partial^2 u}{\partial y^2} + \frac{\partial^2 u}{\partial z^2} = -\frac{P}{\mu}. \tag{2.7}$$

Consider first the rectangular channel $0 \le y \le h$, $0 \le z \le l$. If we write

$$u(y, z) = \frac{1}{2}\frac{Ph^2}{\mu}\left\{\frac{y}{h} - \left(\frac{y}{h}\right)^2\right\} + f(y, z),$$

that is represent the solution as a perturbation of plane Poiseuille flow, then $f(y,z)$ is a harmonic function for which $f=0$ on $y=0,h$ and $f=-(Ph^2/2\mu)\{(y/h)-(y/h)^2\}$ on $z=0,l$. From Boussinesq (1868) we have the solution as

$$u(y,z)=\frac{1}{2}\frac{Ph^2}{\mu}\left\{\frac{y}{h}-\left(\frac{y}{h}\right)^2\right\}$$
$$-\frac{4Ph^2}{\mu\pi^3}\sum_{n=0}^{\infty}\frac{\left[\sinh\left\{\frac{(2n+1)\pi z}{h}\right\}+\sinh\left\{\frac{(2n+1)\pi(l-z)}{h}\right\}\right]\sin\left\{\frac{(2n+1)\pi y}{h}\right\}}{(2n+1)^3\sinh\left\{\frac{(2n+1)\pi l}{h}\right\}}, \tag{2.8}$$

which gives the mass flux along the channel as

$$Q=\int\int_S \rho u(y,z)\,\mathrm{d}y\,\mathrm{d}z=\frac{Ph^3l}{12\nu}-\frac{16Ph^4}{\pi^5\nu}\sum_{n=0}^{\infty}\frac{\left[\cosh\left\{\frac{(2n+1)\pi l}{h}\right\}-1\right]}{(2n+1)^5\sinh\left\{\frac{(2n+1)\pi l}{h}\right\}}. \tag{2.9}$$

From (2.8) and (2.9) the results for plane Poiseuille flow may be recovered in the limit $l\to\infty$. Rowell and Finlayson (1928) also considered the channel of rectangular cross-section with one of the bounding walls moving in the flow direction. This may be considered as a generalisation of the Couette–Poiseuille flow (2.4).

Triangular cross-sections have also received attention. Boussinesq (1868) considered polynomial solutions of the form

$$u(y,z)=-\frac{P}{4\mu h}(y-h)(y-az)(y-bz),$$

which vanishes on the three sides of a triangle. Direct substitution in (2.7) shows at once that $a=-b=\sqrt{3}$ is the only possibility; thus the triangle is an equilateral triangle of side $2h/\sqrt{3}$, with

$$u=-\frac{P}{4\mu h}(y-h)(y^2-3z^2).$$

The corresponding mass flux is given by

$$Q=\frac{Ph^4}{60\sqrt{3}\nu}. \tag{2.10}$$

Proudman (1914) considered the flow in the right-angled isosceles triangle $y=\pi$, $y\pm z=0$, to find

$$u(y,z)=\frac{P}{2\mu}(y+z)(\pi-y)-\frac{P}{\pi\mu}\sum_{n=0}^{\infty}\frac{1}{(n+\frac{1}{2})^3\sinh\{(2n+1)\pi\}}$$
$$\times[\sinh\{\left(n+\tfrac{1}{2}\right)(2\pi-y+z)\}\sin\{\left(n+\tfrac{1}{2}\right)(y+z)\}-\sinh\{\left(n+\tfrac{1}{2}\right)(y+z)\}$$
$$\times\sin\{\left(n+\tfrac{1}{2}\right)(y-z)\}], \tag{2.11}$$

so that

$$Q = \frac{P}{2\nu}\left\{\frac{\pi^4}{6} - \frac{1}{\pi}\sum_{n=0}^{\infty}[\coth\{(2n+1)\pi\} + \operatorname{cosec}\{(2n+1)\pi\}]\left(n+\tfrac{1}{2}\right)^{-5}\right\}. \tag{2.12}$$

2.2 Beltrami flows and their generalisation

Flows associated with the name of Beltrami (1889) (though Truesdell (1954, section 52) notes that nearly all the work of Beltrami had been anticipated by Gromeka (1881)) are those for which $\mathbf{v} \wedge \boldsymbol{\omega} = \mathbf{0}$ so that $\boldsymbol{\omega} = \alpha\mathbf{v}$ for some scalar function α. In that case the vorticity equation (1.7) reduces to

$$\frac{\partial \boldsymbol{\omega}}{\partial t} = \nabla \wedge \mathbf{F} + \nu\nabla^2\boldsymbol{\omega}, \tag{2.13}$$

so that, as noted by Trkal (1919), the only steady Beltrami flows of a viscous fluid, apart from those that are irrotational, are those sustained by a non-conservative body force. Otherwise the vorticity satisfies the diffusion equation and decays. We shall consider unsteady Beltrami flows in chapter 4. A generalisation of Beltrami flows requires, not $\mathbf{v} \wedge \boldsymbol{\omega} = \mathbf{0}$ but

$$\nabla \wedge (\mathbf{v} \wedge \boldsymbol{\omega}) = \mathbf{0} \tag{2.14}$$

which for steady flow, in the absence of any non-conservative body force, also requires from (1.7)

$$\nabla^2\boldsymbol{\omega} = \nabla \wedge \nabla \wedge \boldsymbol{\omega} = \mathbf{0}. \tag{2.15}$$

If we introduce the stream function ψ, as in equation (1.14), such that $\mathbf{v} = \nabla \wedge (\psi\mathbf{k})$ then, with $\boldsymbol{\omega} = (0, 0, \zeta)$ we have, from equation (2.14),

$$\frac{\partial}{\partial x}\left(\zeta\frac{\partial\psi}{\partial y}\right) - \frac{\partial}{\partial y}\left(\zeta\frac{\partial\psi}{\partial x}\right) = 0. \tag{2.16}$$

Further, as noted in (1.15), we have

$$\frac{\partial^2\psi}{\partial x^2} + \frac{\partial^2\psi}{\partial y^2} = -\zeta, \tag{2.17}$$

and equation (2.15) requires

$$\frac{\partial^2\zeta}{\partial x^2} + \frac{\partial^2\zeta}{\partial y^2} = 0. \tag{2.18}$$

The solution of equation (2.16) is

$$\zeta = -f(\psi). \tag{2.19}$$

An exact solution of the Navier–Stokes equations results when the three equations (2.17) to (2.19) are compatible. A special case is when $f(\psi) = K$, a constant, and the equations then reduce to

$$\frac{\partial^2 \psi}{\partial x^2} + \frac{\partial^2 \psi}{\partial y^2} = K, \tag{2.20}$$

which corresponds to a flow in which vorticity is uniform. Such a flow, with uniform vorticity, is a shear flow, with a linearly varying velocity $u(y)$, say, to which we may add a potential flow. Tsien (1943), in his study of the shear flow past aerofoils, gave the solution for a line source and a line vortex, respectively, embedded in such a shear flow as

$$\psi = ay + by^2 + c \tan^{-1}\left(\frac{y}{x}\right), \tag{2.21}$$

$$\psi = ay + by^2 + c \ln(x^2 + y^2), \tag{2.22}$$

for constants a, b, c, whilst Wang (1990b) presented the solution

$$\psi = ay^2 + b\, \mathrm{e}^{-\lambda y} \cos \lambda x, \tag{2.23}$$

with λ constant, which he interpreted in terms of a shear flow over convection cells.

A further solution given by Wang (1991) is

$$\psi = y(ay + bx), \tag{2.24}$$

which may be interpreted as the oblique impingement of two flows for which $y = 0$, $y = -bx/a$ are the dividing streamlines.

The solutions (2.21) to (2.24) are, of course, trivial in the sense that they do not involve the viscosity. Wang (1991) showed that the above range of solutions may be generalised by writing

$$\zeta = \psi + B(x, y),$$

and assuming that B is linear so that $B(x, y) = ax + by$ (in fact Wang has $a \equiv 0$); the vorticity equation (1.17) then yields, as an equation for ψ,

$$\frac{\partial^2 \psi}{\partial x^2} + \frac{b}{\nu}\frac{\partial \psi}{\partial x} = -\left(\frac{\partial^2 \psi}{\partial y^2} - \frac{a}{\nu}\frac{\partial \psi}{\partial y}\right). \tag{2.25}$$

As we see, this equation retains both the viscous diffusion terms and the linearised convection terms; in that sense equation (2.20) is a special case. Solutions of the linear equation (2.25), which embrace a wide selection of recorded exact solutions of the Navier–Stokes equations, are available by the method of separation of variables. Thus, if we set $\psi(x, y) = F(x)G(y)$ then F, G

respectively, satisfy

$$\frac{\mathrm{d}^2F}{\mathrm{d}x^2} + \frac{b}{\nu}\frac{\mathrm{d}F}{\mathrm{d}x} - CF = 0, \quad \frac{\mathrm{d}^2G}{\mathrm{d}y^2} - \frac{a}{\nu}\frac{\mathrm{d}G}{\mathrm{d}y} + CG = 0, \tag{2.26}$$

where C is the separation constant. We consider now the consequences of (2.26) in several special cases.

2.2.1 Flow downstream of a grid

If we take $a = 0$, $b = -U$ and a positive separation constant $C = \lambda^2$ then we have

$$G = A\sin\lambda y \quad \text{and} \quad F = \exp\left[\left\{U/\nu\lambda \pm \sqrt{\left(U^2/\nu^2\lambda^2 + 4\right)}\right\}\lambda x/2\right].$$

Choosing, now, the solution that decays in the x-direction, and setting $\lambda = 2\pi/h$ gives

$$\psi = Uy + A\sin(2\pi y/h)\exp\left[\left\{R - \sqrt{(R^2 + 16\pi^2)}\right\}x/2h\right], \tag{2.27}$$

where $R = Uh/\nu$ is the Reynolds number. Kovásznay (1948) obtained this solution which he suggested may be used to describe the flow downstream from a two-dimensional grid with grid spacing h. With $R = 40$ the streamlines for one period are shown in figure 2.2.

In an extension of this Lin and Tobak (1986) take $C = -\lambda^2 < 0$. If we again set $\lambda = 2\pi/h$, then Lin and Tobak's solution may be written as

$$\psi = Uy + A\exp\left[-2\pi y/h + \left\{R + \sqrt{(R^2 - 16\pi^2)}\right\}x/2h\right]. \tag{2.28}$$

Lin and Tobak interpret this solution as the flow over the permeable plate $y = 0$, $x < 0$ at which suction is applied, noting that for sufficiently large values of A/U there will be flow reversal. However, it should also be noted that the solution (2.28) does not satisfy the no-slip condition at the plate.

A slightly more general solution than (2.28) has

$$\psi = Uy - A\sinh(2\pi y/h)\exp\left[\left\{R + \sqrt{(R^2 - 16\pi^2)}\right\}x/2h\right],$$

which Wang (1966) interprets as a uniform stream encountering a rotational, diverging counterflow.

2.2.2 Flow due to a stretching plate

We now take $a = -U$, $b = 0$ and the separation constant $C = 0$ so that, in general, the solution for ψ is

$$\psi = Ux + (-Ux + k_1)(k_2 + k_3\,\mathrm{e}^{-Uy/\nu}).$$

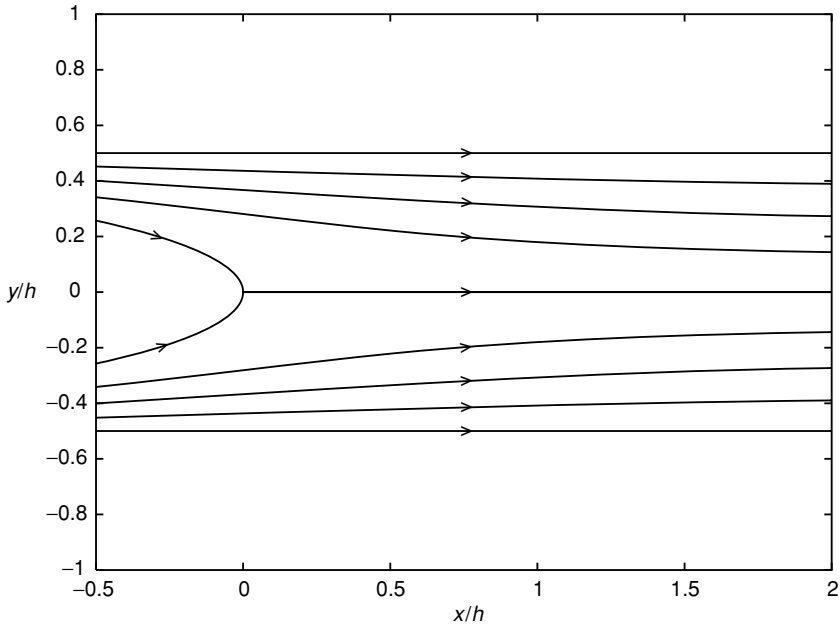

Figure 2.2 Streamlines of the flow represented by equation (2.27) with $A = -(2\pi)^{-1}$ and $R = 40$.

Applying the boundary conditions $\partial\psi/\partial x = 0$ on $y = 0$, $\partial\psi/\partial y = 0$ on $x = 0$ and $\partial\psi/\partial x \to -U$ as $y \to \infty$ gives

$$\psi = Ux(1 - \mathrm{e}^{-Uy/\nu}). \tag{2.29}$$

With

$$u = (U^2 x/\nu)\,\mathrm{e}^{-Uy/\nu} \quad \text{and} \quad v = U(\mathrm{e}^{-Uy/\nu} - 1),$$

we have a flow in the half-plane $y \geq 0$ with fluid speed $U^2 x/\nu$ along the boundary $y = 0$. The solution (2.29) was discovered by Riabouchinsky in 1924, noted in passing as an exact solution in a quite different context by Stuart (1966a) and interpreted by Crane (1970) as the flow due to the stretching plate $y = 0$. Note how vorticity created at the stretching plate is confined to a region of thickness $O(\nu/U)$, beyond which we have uniform flow towards it. Danberg and Fansler (1976) have introduced a uniform flow parallel to the plate, whilst Wang (1984) has extended the analysis to the case in which the plate stretches in orthogonal directions.

McLeod and Rajagopal (1987) have established the uniqueness of this solution, a practical application of which we shall encounter in the next section.

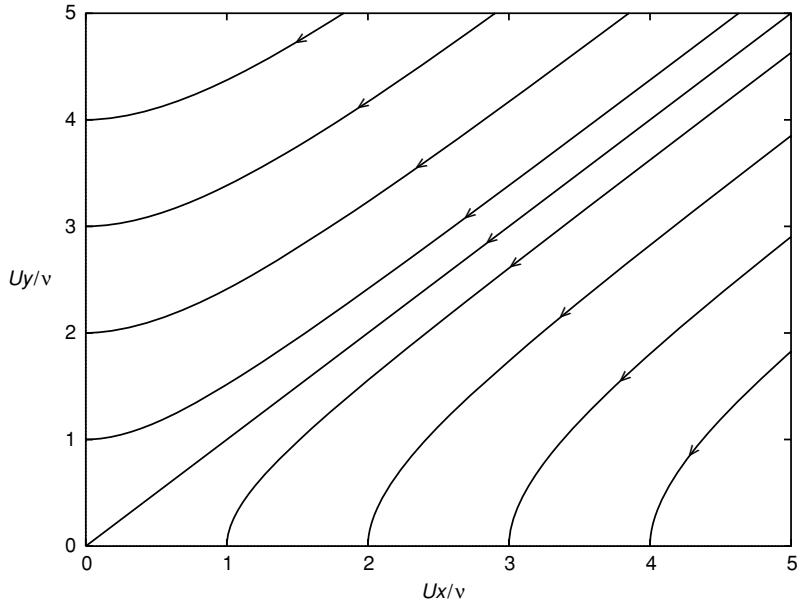

Figure 2.3 The corner flow streamlines represented by equation (2.30).

2.2.3 Flow into a corner

With $a = -U$, $b = U$ and $C = 0$ we have, as the solution which satisfies the no-slip condition on $x = y = 0$, for the flow in the quarter-plane $x, y \geq 0$, bounded as $x, y \to \infty$,

$$\psi = U(x - y) + \nu(\mathrm{e}^{-Ux/\nu} - \mathrm{e}^{-Uy/\nu}). \tag{2.30}$$

At large distances from the bounding walls the streamlines are given by the parallel lines $y = x +$ constant. With

$$u = -U(1 - \mathrm{e}^{-Uy/\nu}) \quad \text{and} \quad v = -U(1 - \mathrm{e}^{-Ux/\nu}),$$

we see that the no-slip condition is satisfied at each of the boundaries, which are permeable, and at each of which there is suction. The streamline pattern is shown in figure 2.3. The solution (2.30) is a special case of a more general class of solutions considered by Berker (1963, section 15).

2.2.4 The asymptotic suction profile

A solution closely related to (2.30) is obtained by taking $a = -V$, $b = -U$, $C = 0$. The solution of (2.25), in the half-plane $y \geq 0$ and bounded at infinity,

which satisfies the no-slip condition on $y = 0$ is

$$\psi = Vx + Uy + \frac{Uv}{V}\mathrm{e}^{-Vy/v}, \tag{2.31}$$

for which $u = U(1 - \mathrm{e}^{-Vy/v})$, $v \equiv -V$. The solution (2.31) corresponds, therefore, to uniform flow over an infinite porous plate at which the suction velocity has magnitude V.

This solution may be interpreted as the steady flow far downstream from the leading edge of a semi-infinite porous flat plate. In the absence of suction, the vorticity created at the surface would diffuse indefinitely as we go downstream. The presence of suction inhibits this and the balance between convection and diffusion, represented by the solution (2.31), confines the vorticity, as in the two previous examples, to a layer of thickness $O(v/U)$.

2.3 Stagnation-point flows

2.3.1 The classical Hiemenz (1911) solution

When a steady stream of a viscous fluid approaches a rigid stationary cylinder, the stream is brought to rest at the surface of the body and divides about it. Although the fluid is at rest, at each point of the surface of the cylinder, by analogy with the flow of an inviscid fluid, we identify stagnation points as those points on the surface at which the stream attaches to, or separates from, the cylinder. The flow in the neighbourhood of a stagnation point of attachment may be modelled by the flow towards an infinite rigid flat plate. Now, for an inviscid fluid, the irrotational flow against the flat plate $y = 0$ is well known to be $u = kx$, $v = -ky$. The constant k is not directly relevant to the flow pattern close to the stagnation point, and is proportional to the free-stream speed about the cylinder. The inviscid stream function is $\psi = kxy$. In his study of the flow of a viscous fluid at a stagnation point it would appear to have been natural for Hiemenz (1911) to have assumed $\psi(x, y) = xF(y)$. If we introduce dimensionless variables, noting that there is no natural length scale in this problem, then

$$\psi = (vk)^{1/2} x f(\eta) \quad \text{where} \quad \eta = \left(\frac{k}{v}\right)^{1/2} y, \tag{2.32}$$

and from (1.17) we have, as the equation for f,

$$f^{iv} + ff''' - f'f'' = 0, \tag{2.33}$$

where a prime denotes differentiation with respect to η, together with the

boundary conditions

$$f(0) = f'(0) = 0, \quad f'(\infty) = 1. \tag{2.34}$$

Integrating (2.33) once gives

$$f''' + ff'' - f'^2 + 1 = 0, \tag{2.35}$$

and from (1.9), (1.10) we may infer that the pressure

$$\frac{p_0 - p}{\rho} = \frac{1}{2}k^2x^2 + \frac{1}{2}\nu k f^2 + \nu k f', \tag{2.36}$$

where p_0 is a constant. Unlike the previous solutions of section 2.2 the present solution describes a flow in which linear diffusion of vorticity is balanced by *non-linear* convection of vorticity. The solution of (2.35), subject to the conditions (2.34), has been calculated numerically by Hiemenz (1911) and by Howarth (1934).

Rott (1956) extended the solution of Hiemenz to include the situation in which the plane boundary slides in its own plane in the x-direction. This provides, for example, a model of the flow in the neighbourhood of the stagnation point of a rotating circular cylinder placed in a uniform stream. In place of (2.32) we have

$$\psi = (\nu k)^{1/2} x f(\eta) + u_w \left(\frac{\nu}{k}\right)^{1/2} \int_0^\eta g \, \mathrm{d}\eta, \tag{2.37}$$

where u_w is the speed of the translating plate. With p unchanged as in (2.36), equation (1.9) then yields, as equation for g,

$$g'' + fg' - f'g = 0 \quad \text{with} \quad g(0) = 1, \quad g(\infty) = 0. \tag{2.38}$$

Rott identifies the solution of (2.38) as $g = f''(\eta)/f''(0)$. In other words the superimposed cross flow is proportional to the shear distribution of the Hiemenz flow. In figure 2.4 we show both $f'(\eta)$ and $g(\eta)$.

An investigation by Becker (1976) provides a novel application of the Hiemenz type of flow. Becker considers the situation in which a film of liquid, of constant thickness h, flows away from the stagnation point on a cylindrical surface with constant radius of curvature R_c, and a horizontal axis. The film is sustained by rain falling with constant speed V; the 'rain' is modelled as a homogeneous medium with density $\epsilon\rho$, where ρ is the liquid density and $0 < \epsilon < 1$. If α is the angle of inclination of the tangent of the cylinder surface to the horizontal, and x is measured from the stagnation point along the surface, then $\alpha = x/R_c$ and Becker makes the assumption $\alpha \ll 1$.

In this problem we have a body force per unit mass $Y\mathbf{j} = -g\mathbf{j}$, so that in (1.9), (1.10) it is convenient to work with the modified pressure $p^* = p + \rho g y$.

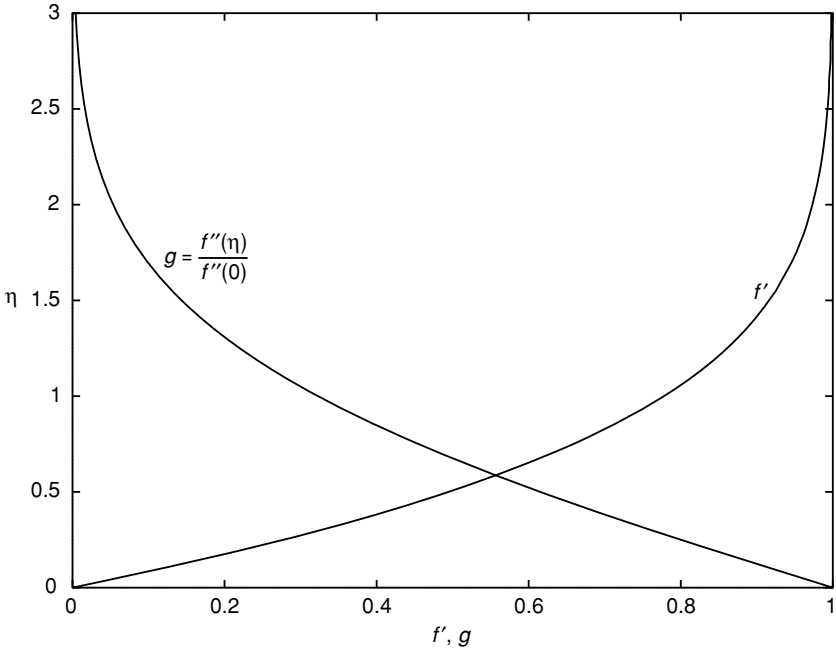

Figure 2.4 The stagnation-point velocity profile $f'(\eta)$, and the cross-flow profile $g(\eta) = f''(\eta)/f''(0)$.

The same similarity transformation (2.32) as used in the classical Hiemenz flow is adopted but now, in addition to the standard conditions at the boundary, we must consider conditions at the interface $y = h$. If we define $\eta_h = (k/\nu)^{1/2}h$ then mass conservation requires

$$f(\eta_h) = \epsilon V/(\nu k)^{1/2}. \tag{2.39}$$

The balance of tangential momentum at the interface, in the formal limit $R_c \to \infty$, requires

$$f''(\eta_h) + f(\eta_h)f'(\eta_h) = 0. \tag{2.40}$$

For the pressure note that as before we have

$$\frac{p^*}{\rho} = \frac{1}{2}bx^2 - \frac{1}{2}\nu k f^2 - \nu k f', \tag{2.41}$$

where we have set $p_0 = 0$, and b is, as yet, undetermined. A consideration of the balance of momentum normal to the interface leads to the result that $b = -g/R_c$, where higher powers of R_c^{-1} have been ignored. We now define a Reynolds number $Re = (gR_c)^{1/2}R_c/\nu$ and a Froude number $Fr = \epsilon V/(gR_c)^{1/2}$.

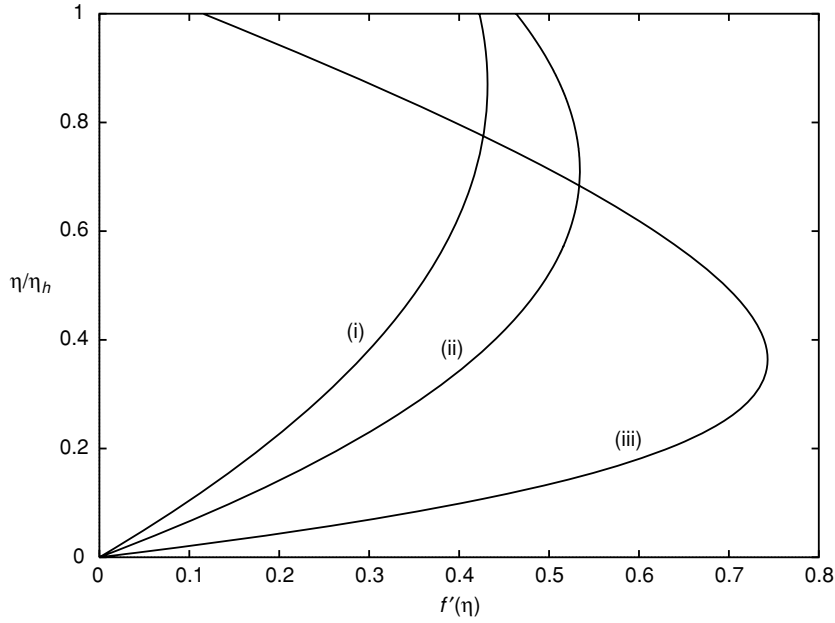

Figure 2.5 Solutions of equation (2.42) corresponding to (i) $\lambda = 1.2$, (ii) $\lambda = 1.0$, (iii) $\lambda = 0.8$.

If in the limit $R_c \to \infty$, $FrRe^{1/2} \to \beta$, a constant, then we have an exact solution of the Navier–Stokes equations where $f(\eta)$ satisfies

$$f''' + ff'' - f'^2 + \lambda = 0, \tag{2.42}$$

where λ is determined from β. This equation is to be solved subject to $f(0) = f'(0) = 0$, and the interface condition (2.40). Some typical velocity profiles are shown in figure 2.5.

Becker's analysis included finite curvature effects, as the model of a road, for which the above may be considered as the leading term in an appropriate expansion.

2.3.2 Oblique stagnation-point flows

In section 2.3.1 above, the dividing, or stagnation, streamline intersects the plane boundary $y = 0$ orthogonally. There is, however, a class of stagnation-point flows for which the dividing streamline intersects the boundary at an arbitrary angle. Consider first an inviscid fluid and the stream function

$$\psi = kxy + \tfrac{1}{2}\zeta_0 y^2, \tag{2.43}$$

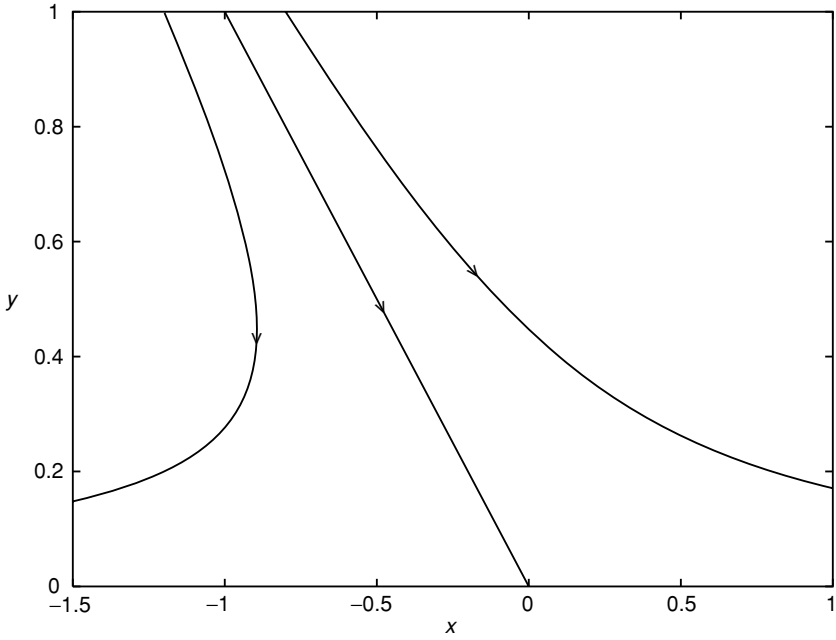

Figure 2.6 Streamlines for oblique inviscid stagnation-point flow, from equation (2.43) with $\zeta_0 = 2k$.

which combines both the classical stagnation-point flow and a cross flow of uniform shear, that is of constant vorticity $-\zeta_0$. This stream function satisfies both the Euler equations and the Navier–Stokes equations, though not the viscous condition of no slip at $y = 0$. Taking $y = 0$ as the boundary again, we see from (2.43) that the dividing streamline is now $y = -2(k/\zeta_0)x$ and the flow is sketched in figure 2.6.

This form of stagnation-point flow has been developed by Stuart (1959), Tamada (1979) and Dorrepaal (1986) for a viscous fluid as follows. With a superposed cross flow present it is natural, taking account of (2.37) and (2.43), to write the stream function as

$$\psi = (\nu k)^{1/2} x f(\eta) + \zeta_0 \left(\frac{\nu}{k}\right) \int_0^\eta g \, \mathrm{d}\eta, \tag{2.44}$$

where again $\eta = (k/\nu)^{1/2} y$. Substitution of (2.44) into equation (1.17) yields ordinary differential equations for f and g. Integrating each of these once with respect to η results in equation (2.35) for f, whilst for g we have

$$g'' + fg' - f'g = \text{constant}, \tag{2.45}$$

together with $g(0) = 0$, $g'(\infty) = 1$. Now, the solution for f has the property that, as $\eta \to \infty$, $f \sim \eta - A$, where $A = 0.6479$ represents the viscous

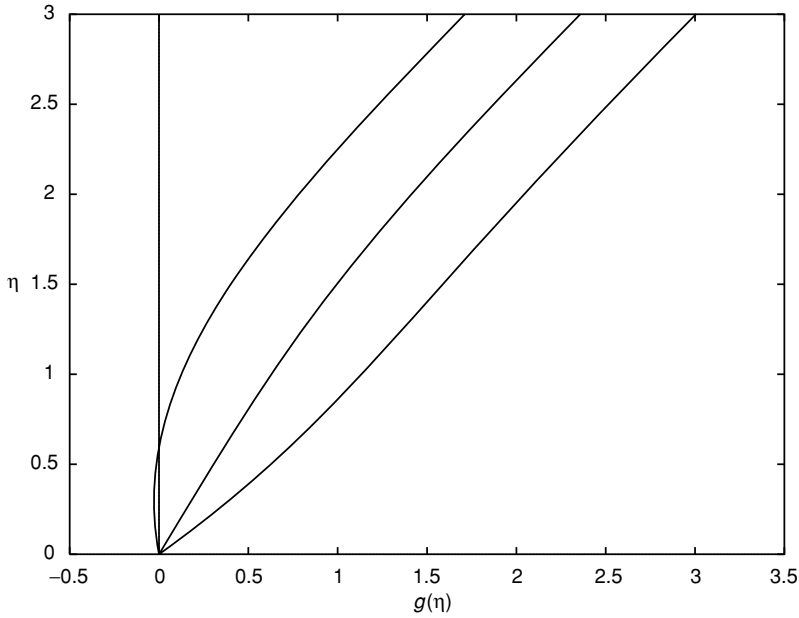

Figure 2.7 Cross-flow velocity profiles $g(\eta)$ for oblique stagnation-point flow with, from the left, $B - A = 0.6479, 0, -0.6479$, respectively.

displacement effect. Similarly we have $g \sim \eta - B$, where B is undetermined, so that (2.45) becomes

$$g'' + fg' - f'g = B - A. \tag{2.46}$$

From equations (1.9) and (1.10) the pressure is given by

$$\frac{p_0 - p}{\rho} = \frac{1}{2}k^2x^2 + \frac{1}{2}\nu k f^2 + \nu k f' - \zeta_0(\nu k)^{1/2}(B - A)x. \tag{2.47}$$

With B arbitrary we see that (2.47) incorporates an additional constant pressure gradient in the x-direction, proportional to $B - A$, the effect of which is, simply, to determine the displacement of the uniform shear flow parallel to the plate. Denoting $g'(0) = D$, where D is known when B is specified, $f''(0) = C = 1.2326$ the solution of equation (2.46) is formally obtained as

$$g(\eta) = (A - B)f'(\eta) + C\{D - C(A - B)\}f''(\eta)\int_0^\eta \{f''(t)\}^{-2} \times \exp\left\{-\int_0^t f(s)\,\mathrm{d}s\right\}\mathrm{d}t. \tag{2.48}$$

In figure 2.7 we show, for various values of $B - A$, profiles $g(\eta)$. In their analyses Stuart and Tamada take $B = A$, and Dorrepaal takes $B = 0$.

From a consideration of the solution (2.44) close to the boundary $y = 0$, it can be shown that the dividing streamline $\psi = 0$ meets the boundary at

$$x = x_s = -\zeta_0 \left(\frac{\nu}{k^3}\right)^{1/2} \left(\frac{D}{C}\right),$$

where its slope is given by

$$-\frac{3kC^2}{\zeta_0\{(B - A)C + D\}},$$

which is independent of the kinematic viscosity ν. Furthermore, the ratio of this slope to that of the dividing streamline far from the boundary, where viscous effects are unimportant, is

$$\frac{3}{2}\frac{C^2}{\{(B - A)C + D\}}$$

which is, in addition, independent of k and ζ_0, depending only upon the constant pressure gradient parallel to the boundary through both B and D.

2.3.3 Two-fluid stagnation-point flow

The classical Hiemenz stagnation-point flow is that of a stream against a solid boundary. Wang (1985a) has extended this to the flow against the interface with a second fluid. The interface is assumed planar so that we may expect the surface tension to be large, or the density of the lower fluid to be much greater than the density of the upper fluid.

The similarity of the Hiemenz flow is preserved so that in the upper fluid the stream function is expressed as in (2.32), with $f(\eta)$ again satisfying equation (2.35). However the no-slip condition is violated in this case and we have $f'(0) = \lambda$, where λ is determined only following a consideration of the flow in the second fluid in $y < 0$. In the second fluid, which we assume has density $\bar{\rho}$ and viscosity $\bar{\mu}$, we write

$$\bar{\psi} = -(\bar{\nu}k\lambda)^{1/2} x \bar{f}(\bar{\eta}) \quad \text{where now} \quad \bar{\eta} = -\left(\frac{k\lambda}{\bar{\nu}}\right)^{1/2} y. \tag{2.49}$$

Since we require $\bar{f}'(\infty) = 0$, where a prime again denotes differentiation with respect to the independent variable, the equation for $\bar{f}$ is

$$\bar{f}''' + \bar{f}\,\bar{f}'' - \bar{f}'^2 = 0, \quad \bar{f}(0) = 0, \quad \bar{f}'(0) = 1, \quad \bar{f}'(\infty) = 0. \tag{2.50}$$

Where the conditions at $\bar{\eta} = 0$ ensure continuity of velocity at the interface. The solution of (2.50) is

$$\bar{f}(\bar{\eta}) = 1 - \mathrm{e}^{-\bar{\eta}}.$$

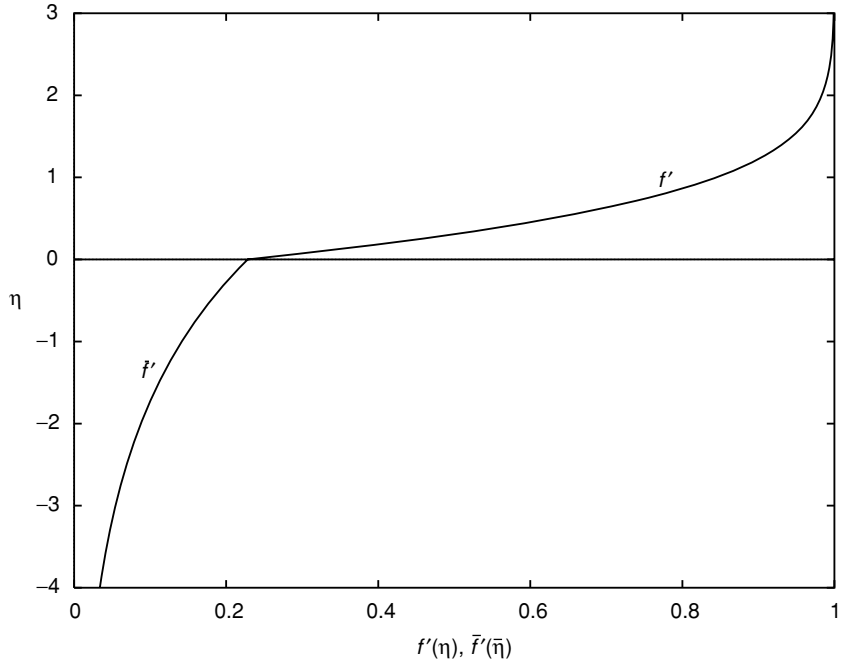

Figure 2.8 Tangential velocity profile for a two-fluid stagnation-point flow.

This solution we have met before in equation (2.29). There, as remarked, Crane (1970) interpreted it as the flow due to a stretching plate. Whilst this might be difficult to envisage physically, in the present context the 'stretching plate' is simply the free surface at which the velocity does increase linearly with distance. To complete the solution the parameter λ must be determined, and this is possible from continuity of stress at the interface from which we have

$$\frac{f''(0)}{\lambda^{3/2}} = \frac{\bar{\rho}}{\rho}\left(\frac{\bar{\nu}}{\nu}\right)^{1/2}, \tag{2.51}$$

so that λ may be determined from the numerical solution of (2.35), (2.51). For a two-fluid system with water over olive oil we have, in cgs units, $\rho = \bar{\rho} = 1$, $\nu = 0.0114$, $\bar{\nu} = 1.0$, and find $\lambda = 0.22841$. The tangential velocity profile is shown in figure 2.8.

Wang (1987) has also considered the impingement of two stagnation-point flows at a two-fluid interface, whilst Tilley and Weidman (1998) have extended Wang's analysis to oblique stagnation-point flow in a two-fluid system.

2.4 Channel flows

At the beginning of this chapter we considered the flow in parallel-sided channels, typical of which is the classical Couette–Poiseuille flow. With a cross flow in the channel due to equal suction and injection at the boundaries, convective terms were retained, but only linearly. We now consider channel flows in which the non-linear terms can be neither neglected nor linearised.

2.4.1 Parallel-sided channels

Consider first the flow in a channel with plane porous walls, $y = \pm h$, across which fluid is injected or extracted with constant uniform velocity V. This problem first attracted the attention of Berman (1953). With $\overline{x} = x/h, \quad \overline{y} = y/h$ the stream function is written as

$$\psi = h(U_0 - V\overline{x})f(\overline{y}), \tag{2.52}$$

where U_0 is an arbitrary velocity. With $\mu V/h$ as a scale for the pressure we have

$$\overline{p} = f' - \tfrac{1}{2}Rf^2 - \tfrac{1}{2}\lambda\overline{x}^2 + K\overline{x}, \tag{2.53}$$

where $R = Vh/\nu$ is the Reynolds number, positive for suction and negative for injection, λ is a parameter to be determined and $K = U_0\lambda/V$. We note that U_0 has no significant role to play, being simply the result of a constant pressure gradient along the channel. From (1.9), (2.52) and (2.53) we have, as the equation for f,

$$f''' + R(f'^2 - ff'') - \lambda = 0, \tag{2.54}$$

and if the flow is assumed to be symmetrical about the channel centre-line the boundary conditions are

$$f(0) = f''(0) = 0, \quad f(1) = 1, \quad f'(1) = 0.$$

That four conditions are required reflects the fact that λ is not determined *a priori*.

Berman (1953) constructed solutions of (2.54) for $|R| < 1$, whilst Yuan (1956) concentrated on the case $|R| \gg 1$. Terrill (1964, 1965) extended Berman's results, determined solutions numerically for $R = O(1)$, and on re-examining Yuan's results for $|R| \gg 1$ concluded they were valid only for $R < 0$, and then with anomalous behaviour at $\overline{y} = 0$ which he corrected, as well as considering the case $R \gg 1$. As $|R| \to \infty$ a boundary layer forms, either at $\overline{y} = 1$ with thickness $O(R^{-1})$ for $R > 0$, or at $\overline{y} = 0$ with thickness $O(|R|^{-1/2})$ for $R < 0$. Dual solutions were observed by Raithby (1971)

for $R > 12$ but it was Robinson (1976) who uncovered the flow structure in greater detail. Thus, with $R > 0$ there are Type I solutions for which the velocity maximum is on the centre-line $\overline{y} = 0$, which are the solutions obtained by Terrill. For $R < 12.165$ these are the only solutions available, but when $R > 12.165$ two further solutions emerge. When $R > 13.119$ there are Type II solutions for which $f'(\overline{y}) > 0$, with the maximum velocity located between the centre-line and solid boundary. And finally there are Type III solutions. For $12.165 < R < 13.119$ there are dual solutions of this type, characterised by $f'(0) < 0$ and a region of reversed flow beyond which the velocity is positive. For $R > 13.119$ these Type III solutions continue to display the same characteristics. As $R \to \infty$, Type I and II solutions are virtually indistinguishable, differences being attributed to exponentially small terms. In figure 2.9 these features are illustrated.

Robinson confined his attention to values of $R > 0$, whereas Terrill's original (1964) investigation included values of $R < 0$, a continuation of the solutions now labelled Type I. It may be noted that Skalak and Wang (1978) have proved that there is at most one such solution whilst Shih (1987) has established the existence of a solution for all $R < 0$. In a penetrating analysis of the problem, Zaturska, Drazin and Banks (1988) have shown that when $R > 0$ bifurcations occur at $R = 6.001353$ on the Type I solution branch and at $R = 15.4146$ on the Type III solution branch. Each of these implies the existence of asymmetric solutions in the neighbourhood of each bifurcation point. Asymmetric solutions occur more naturally if the porous boundaries have different permeabilities, that is the suction and/or injection velocities are different at each boundary. In a series of papers Terrill and Shrestha (1965), and Shrestha and Terrill (1968), have considered such problems when there is suction or injection across each boundary, or suction at one and injection at the other, including the situation in which one wall is impermeable. Analyses for $R \ll 1$, $R \gg 1$ are complemented by numerical solutions.

Cox (1991a) continues the asymmetric solutions of the symmetric problem to derive new solutions of the asymmetric problem. In particular Cox (1991b) considers the situation in which one wall is impermeable. A generalisation of the problem originally posed by Berman, to three-dimensional flow, has been considered by Taylor, Banks, Zaturska and Drazin (1991).

In a problem, not unrelated to some of those considered in section 2.3, at least in the sense that stretching boundaries are involved, Brady and Acrivos (1981) consider the flow in a channel due to the stretching of its boundaries. Although this is an idealised problem the motivation was provided from the study of the flow within a long slender drop located in an extensional flow.

Specifically, Brady and Acrivos consider a channel $-h \leq y \leq h$ whose (impermeable) boundaries each move in their own plane with speed $U_0 x/h$.

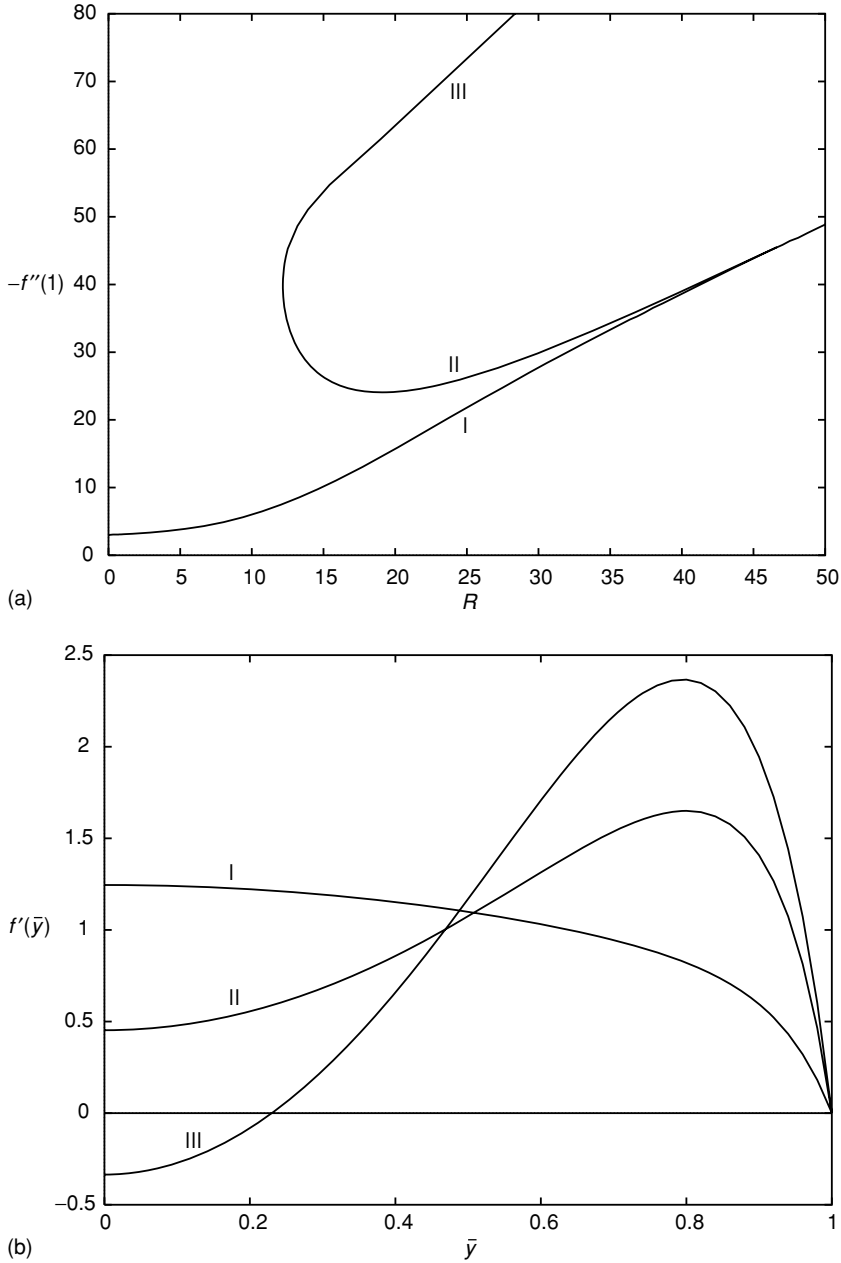

Figure 2.9 (a) Variation of $f''(1)$ with R for $R > 0$. (b) Velocity profiles for solutions of Type I with $R = 15.0141$, Type II with $R = 14.7151$, and Type III with $R = 12.5609$.

Since the flow is antisymmetric about $x = 0$, and symmetric about $y = 0$, only the flow in $x \geq 0$, $0 \leq y \leq h$ need be considered. Again we set $\overline{x} = x/h$, $\overline{y} = y/h$ and write

$$\psi = U_0 h \overline{x} f(\overline{y}), \tag{2.55}$$

which is essentially the Hiemenz transformation, and with $\mu U_0/h$ as a scale for the pressure we have

$$\overline{p} = \tfrac{1}{2}\lambda \overline{x}^2 - \left(f' + \tfrac{1}{2} R f^2\right), \tag{2.56}$$

where $R = U_0 h/\nu$ is the Reynolds number and, again, λ is to be determined.

From (1.9), (2.55) and (2.56) we find, for $f(\overline{y})$

$$f''' + R(ff'' - f'^2) - \lambda = 0, \tag{2.57}$$

with boundary conditions

$$f(0) = f''(0) = 0, \quad f(1) = 0, \quad f'(1) = 1. \tag{2.58}$$

Numerical solutions of (2.57), subject to (2.58) have been obtained by Brady and Acrivos.

For $R \to 0$ we have $\lambda = 3$, $f = \overline{y}(\overline{y}^2 - 1)/2$; the flow is typical of what one might expect, namely with $f' > 0$ for $\overline{y}_0 < \overline{y} < 1$, where $\overline{y}_0 = 3^{-1/2}$ in this limit, with a reversed core flow for $0 < \overline{y} < \overline{y}_0$, and maximum flow reversal on the centre-line. This solution, designated Type I, varies continuously, with $\lambda \to -1$ as $R \to \infty$, displaying the same features throughout. For $R \gg 1$ the reversed core flow is essentially inviscid and uniform with velocity $O(U_0 R^{-1/2})$, flanked by boundary layers, with classical boundary-layer thickness $O(hR^{-1/2})$, at each boundary. The solution is unique for $R \leq R_c \approx 310$. Beyond $R = R_c$ there are three solutions corresponding to distinct values of λ. On an upper branch we have $\lambda \to -1$ as $R \to \infty$, and these so-called Type II solutions are almost indistinguishable from Type I. However as R decreases interesting new developments appear. The centre-line velocity at first increases, and then decreases until at $R = 337.4$ it vanishes. Meanwhile the maximum reversed core-flow velocity has established itself at $\overline{y} \approx 0.68$. Continuing along this branch, which has $\lambda \to -\infty$ as $R \to \infty$ with $|\lambda| = O(R)$ we have Type III solutions, with the positive centre-line velocity increasing, and the whole region of reversed flow now off the centre-line. Eventually, as $R \to \infty$, an inviscid core flanked by thin, classical boundary layers is again established. It may be noted that for $R > 100$ the shear stresses at $y = 1$ for the three solutions are indistinguishable numerically with $f''(1) = R^{1/2}$.

In this investigation Brady and Acrivos considered only the situation $R > 0$, corresponding to walls accelerating away from the origin. They advanced physical reasons for restricting their choice in this way. Subsequently Durlofsky and Brady (1984) found solutions of Type I for $R < 0$, for which case the walls accelerate towards the origin with outflow in the core. In a comprehensive study of flows of Type I, Watson, Banks, Zaturska and Drazin (1991) have discovered the existence of asymmetric solutions; these manifest themselves via pitchfork bifurcations at $R = 132.75849$ and $R = -17.30715$.

Cox (1991b) has extended the range of solutions to the case in which one wall accelerates whilst the other is at rest. While Watson *et al.* (1991) find additional solutions by combining porous and accelerating boundaries, of which the problem of Becker (1976) might be considered to be a special case.

2.4.2 Non-parallel-sided channels

One of the most celebrated exact solutions of the Navier–Stokes equations is associated with the flow between non-parallel plane walls of included angle 2α. The walls intersect at the origin where there is a source or sink leading to either a diverging or converging flow. The problem was first studied by Jeffery (1915) and Hamel (1916). Subsequently, special aspects of the problem have been addressed by Harrison (1919), von Kármán (1924), Tollmien (1931), Noether (1931) and Dean (1934). However, more comprehensive treatments have been given by Rosenhead (1940), Millsaps and Pohlhausen (1953), Berker (1963) and Whitham (1963). In what follows we adopt the approach of Whitham.

If Q is the volume flux per unit distance perpendicular to the plane of the flow, which may be either positive or negative, then, since it has dimensions L^2/T, $R = Q/\nu$ can be adopted as a Reynolds number. Further, since Q, ν are the only physical parameters of the problem then rv_r/ν and rv_θ/ν must depend upon Q/ν and θ alone. With a similar argument applied to the pressure difference $p - p_0$ we have

$$v_r = \frac{\nu F(\theta)}{r}, \quad v_\theta = \frac{\nu G(\theta)}{r}, \quad \frac{p - p_0}{\rho} = \frac{\nu^2 P(\theta)}{r^2}. \tag{2.59}$$

From the continuity equation (1.22) we have $G(\theta) = \text{constant} \equiv 0$ since $v_\theta = 0$ at the boundaries $\theta = \pm\alpha$. Substitution of (2.59) into (1.19) and (1.20) then yields $P' = 2F'$ so that $P = 2F + C_1$, and $P = -(F^2 + F'')/2$. It follows that F satisfies

$$F'' + F^2 + 4F + 2C_1 = 0,$$

from which, multiplying by F' and integrating, we have

$$\tfrac{1}{2}F'^2 + \tfrac{1}{3}F^3 + 2C_1F = C_2,$$

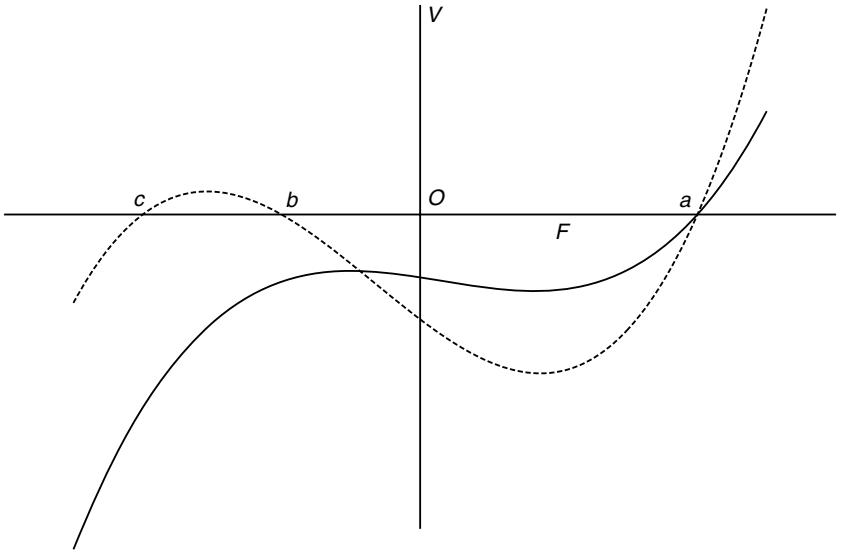

Figure 2.10 A sketch of the two possible forms for $V(F)$.

which in turn may be written as

$$\tfrac{1}{2}F'^2 - \tfrac{1}{3}(a - F)(F - b)(F - c) = 0, \tag{2.60}$$

where the constants a, b, c are related to C_1, C_2, and $a + b + c = -6$. The range and type of solutions available, for which the no-slip condition requires $F(\pm\alpha) = 0$, may be illustrated by a dynamical interpretation of equation (2.60). Thus, with θ as 'time' and F as 'displacement' we may interpret (2.60) as the energy equation for a particle of unit mass, moving on a straight line, whose potential energy is

$$V(F) = -\tfrac{1}{3}(a - F)(F - b)(F - c). \tag{2.61}$$

The total energy is zero and $V \leq 0$ in the motion. Since the particle starts at $F = 0$ for $\theta = -\alpha$, and returns to $F = 0$ for $\theta = \alpha$, there are essentially two situations to consider. The first has b, c complex conjugates with $a > 0$, whilst for the second all are real with $c < b < 0 < a$. These are illustrated in figure 2.10. In the first case the particle starts at $F = 0$ with finite positive velocity, reaches $F = a$ where its velocity is zero but the acceleration $F'' = -\mathrm{d}V/\mathrm{d}F$ is negative, and returns to 0. The motion beyond 0 is of no concern and the particle moves off to infinity. The particle motion in $0 < F < a$ describes a fluid motion that is a pure outflow, since $F > 0$, and symmetric about $\theta = 0$. For the second case the situation is more complex. A motion of the particle from $F = 0$ to $F = a$ returning to $F = 0$ again interprets as symmetric pure

outflow. Correspondingly a motion from $F = 0$ to $F = b$ returning to $F = 0$, with $F < 0$ throughout, interprets as symmetric pure inflow. But now, of course, the particle may oscillate in $b \leq F \leq a$ corresponding to a fluid flow which has both regions of outflow and regions of inflow, with the flow not necessarily symmetric about $\theta = 0$. For each outflow or inflow region the extrema of F are a or b respectively. This rich structure of solutions is summarised by Rosenhead (1940) from whom we quote:

> For every pair of values of α and R the number of mathematically possible velocity profiles of radial motion is infinite.... The profiles may or may not be symmetrical with respect to the central line of the channel. If $\pi > \alpha > \pi/2$ *pure* outflow is impossible, and there is a range of values of small Reynolds number in which *pure* inflow is impossible. The effect of increasing R in outflow is to exclude, progressively, more and more of the simpler types of flow. No such exclusion is introduced when $|R|$ is increased in inflow. With increasing Reynolds number in pure inflow, and with small values of α, the velocity profile exhibits all the well-known characteristics of boundary layers near the walls, and an approximately constant velocity across the rest of the channel. In pure outflow the flow becomes more and more concentrated in the centre of the channel as R is increased, until finally regions of inflow occur near the wall.

In the above context the 'simplest' type of flow is pure outflow or inflow. For pure outflow we have, since $F = a$ when $\theta = 0$, from equation (2.60)

$$\theta = \pm\sqrt{\frac{3}{2}}\int_F^a \frac{\mathrm{d}t}{\sqrt{(a-t)(t-b)(t-c)}}, \tag{2.62}$$

from which we infer that

$$\alpha = \sqrt{\frac{3}{2}}\int_0^a \frac{\mathrm{d}F}{\sqrt{(a-F)(F-b)(F-c)}}, \tag{2.63}$$

and we have

$$\frac{1}{2}R = \sqrt{\frac{3}{2}}\int_0^a \frac{F\,\mathrm{d}F}{\sqrt{(a-F)(F-b)(F-c)}}. \tag{2.64}$$

For pure inflow the limits of integration are from b to F, or 0, in the above. As with the heuristic discussion associated with the dynamics of a single particle, more complicated flows may be deduced from appropriate combinations of these. For given values of α and R the constants a, b, c may, in principle, be determined from (2.63), (2.64) and the constraint $a + b + c = -6$, and the solution completed from (2.62).

Whilst computational methods can complete the solution it is possible to express it in terms of tabulated functions by a suitable transformation. Thus

in the first case with a real and b, c complex conjugates, only pure outflow is possible with

$$F(\theta) = a - \frac{3M^2}{2}\frac{1 - \mathrm{cn}(M\theta, \kappa)}{1 + \mathrm{cn}(M\theta, \kappa)}, \tag{2.65}$$

where $M^2 = 2\{(a-b)(a-c)\}^{1/2}/3$, $2\kappa^2 = 1 + (a+2)/M^2$. For the second case with a, b, c real we have, for outflow,

$$F(\theta) = a - 6k^2m^2\,\mathrm{sn}^2(m\theta, k), \tag{2.66}$$

and for inflow

$$F(\theta) = a - 6k^2m^2\,\mathrm{sn}^2\{K(k^2) - m\theta, k\}, \tag{2.67}$$

where $m^2 = (a-c)/6, k^2 = (a-b)/(a-c)$ and K is the first complete elliptic integral.

The limiting form for pure outflow will have $F'(\pm\alpha) = 0$ which implies, from (2.60), that $b = 0$. In that case we see from (2.63) that the critical value of α, say α_c, is

$$\begin{aligned}\alpha_c &= \sqrt{\frac{3}{2}}\int_0^a \frac{\mathrm{d}F}{\sqrt{F(a-F)(F+a+6)}} \\ &= \sqrt{\frac{3}{2a}}\int_0^1 \frac{\mathrm{d}t}{\sqrt{t(1-t)\{1+(1+6/a)t\}}} = \sqrt{\frac{6}{a}}kK(k^2),\end{aligned} \tag{2.68}$$

with $k^2 = a/\{2(3+a)\}$ in this limiting case, which determines $\alpha_c = \alpha_c(a)$. One may note that $a = rv_r|_{\max}/\nu$ may be interpreted as a Reynolds number of the flow, and is used as such by Millsaps and Pohlhausen (1953). The corresponding critical flux

$$R_c = \frac{Q_c}{\nu} = 2\int_0^{\alpha_c}\{a - 6k^2m^2\,\mathrm{sn}^2(m\theta, k)\}\,\mathrm{d}\theta = 12\frac{\{E(k^2) - (1-k^2)K(k^2)\}}{\sqrt{(1-2k^2)}}, \tag{2.69}$$

where E is the second complete elliptic integral. Since the simplest type of flow is pure inflow or outflow, the critical curve $\alpha_c = \alpha_c(R)$ which places a limit on such flows is of particular importance and is shown in figure 2.11. For $a \gg 1$, $k^2 \sim (1 - 3/a)/2$ and from (2.68), (2.69) we have $\alpha_c \sim 9.42/R$.

For pure inflow, given by (2.67), as $-b$ increases the flow tends to become uniform, except for boundary layers close to the walls. To see this note that m^2 is large and so for given α, bounding θ, K must be large and so $k \approx 1$, $\mathrm{sn}t \approx \tanh t$, $c \approx b$, $a \approx -2b$ and we have

$$F(\theta) = b[3\tanh^2\{(-b/2)^{1/2}(\alpha - \theta) + \beta\} - 2],$$

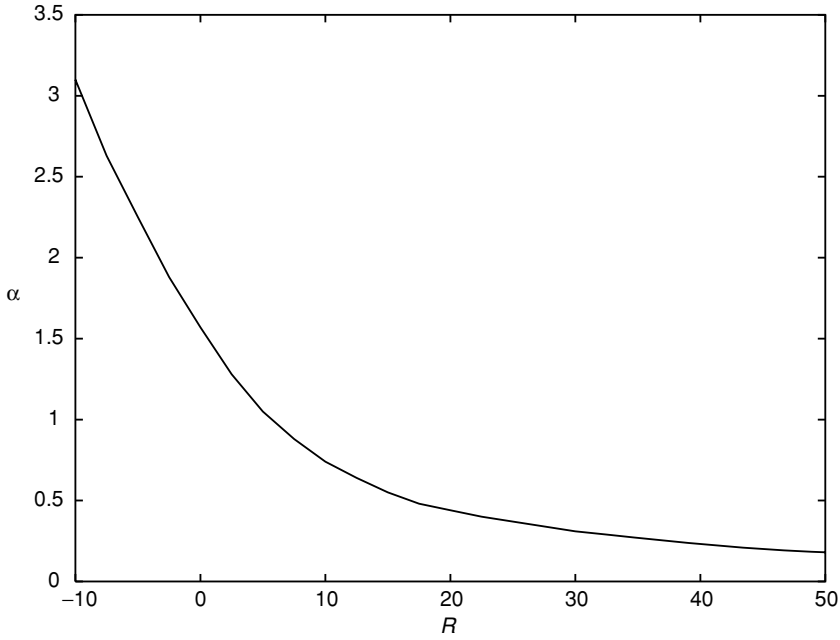

Figure 2.11 The critical curve $\alpha_c = \alpha_c(R)$. Below this pure inflow or outflow is possible, above it regions of reversed flow must be present.

where $\beta = \tanh^{-1}\sqrt{2/3}$, from which we see that $F \approx b$ except in boundary layers of thickness $O\{(-b)^{-1/2}\}$. The volume flux is given by $Q/\nu \approx 2\alpha b$ so that $|R| = O(|b|)$, and the boundary layers have classical thickness $O(|R|^{-1/2})$. In figure 2.12 we show velocity profiles for both diverging and converging flows. These have been obtained by direct numerical integration of the differential equation for F, utilising data set out in Millsaps and Pohlhausen (1953).

The formal requirement that there is a line source, or sink, at the intersection of the plane boundaries appears to limit the usefulness of the Jeffery–Hamel flows. However, Fraenkel (1962, 1963) has demonstrated their applicability to flows bounded by slightly curved walls, originating from a channel of non-vanishing width. The walls are required to turn smoothly, and the 'slightly curved' condition demands that

$$\kappa = \text{local wall curvature} \times \text{local channel width} \ll 1.$$

There is no restriction on the local angle α the wall makes with the channel centre -line. With these requirements satisfied, Fraenkel (1962) shows that a Jeffery–Hamel solution based on the local divergence angle, α, and volume flow through the channel, Q, provides a first approximation to the exact solution at every

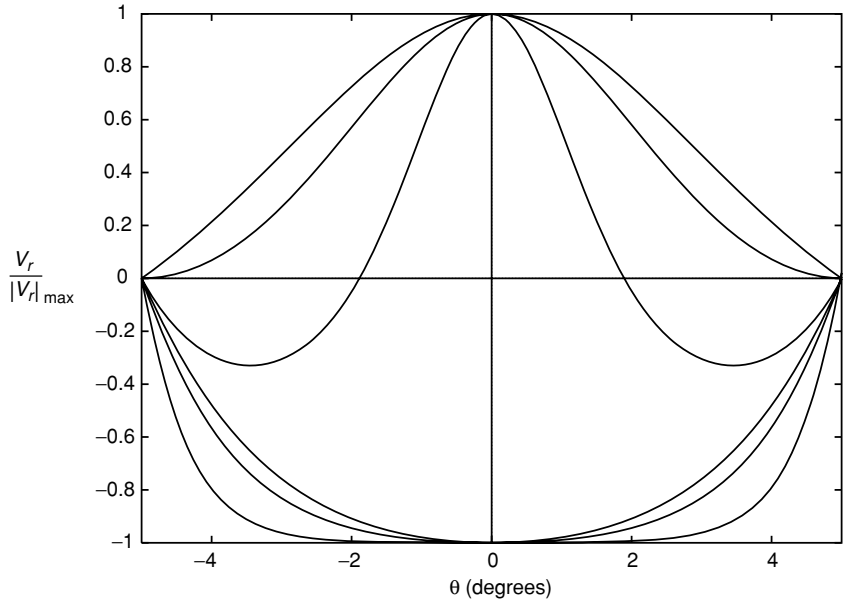

Figure 2.12 Velocity profiles for inflow and outflow in a channel of included angle 10°. If a Reynolds number $R_m = r v_r|_{\max}/\nu$ is defined then, from the bottom, the profiles correspond to $R_m = -5000, -1342, -684, 5000, 1342, 684$, respectively.

station $r =$ constant, With this as the leading term Fraenkel (1963) develops the solution in series form. One aim of these investigations is the construction of solutions of the Navier–Stokes equations, in channels of varying width, which involve flow separation.

Generalisations of the classical case have been considered when a normal velocity proportional to distance from the vertex is imposed on both boundaries (Moffatt and Duffy (1980)), and to the case in which the viscosity and density are arbitrary functions of θ (Hooper, Duffy and Moffatt (1982)).

In Hamel's (1916) investigation the flow between non-parallel plane walls emerged as a special case of spiral flow between solid walls, where the results are similar to those obtained above. In his study of spiral flows he showed, in particular, that streamlines in the form of equiangular spirals are the only streamlines which can coincide with the streamlines of a potential flow without the motion itself being irrotational. An extensive account of the work by Hamel may be found in Berker (1963).

In a related problem Berker (1963), and most recently Putkaradze and Dimon (2000), consider flows of the form (2.59), (2.60) in the absence of any boundaries. Such a flow corresponds to a non-uniform two-dimensional source. In

particular Putkaradze and Dimon, seeking solutions with k-fold symmetry with respect to θ, show that solutions only exist for $R \leq \pi(k^2 - 4)$, a result also given by Goldshtik and Shtern (1989). Putkaradze (2003) also considers the radial flow, from a two-dimensional source, of two immiscible fluids separated by radial lines. In that case the boundary conditions of the classical flow are replaced by conditions of continuity of velocity and stress at the fluid–fluid interfaces.

2.5 Three-dimensional flows

In this section we consider flows that take place not solely in the (x, y)-plane, but also have a component of velocity in the z-direction.

2.5.1 A corner flow

Stuart (1966b) considers flows for which the velocity components $u = \phi_x$, $v = \phi_y$ where $\phi = \phi(x, y)$ is a velocity potential with $\nabla^2\phi = 0$, and $w = w(x, y)$. With the pressure p given by $p/\rho = -(\phi_x^2 + \phi_y^2)/2$, equations (1.9) (1.10) are, in the absence of any body force, satisfied identically and, from (1.11), w satisfies

$$\frac{\partial\phi}{\partial x}\frac{\partial w}{\partial x} + \frac{\partial\phi}{\partial y}\frac{\partial w}{\partial y} = \nu\left(\frac{\partial^2 w}{\partial x^2} + \frac{\partial^2 w}{\partial y^2}\right),$$

with solution

$$w = A + B\,\mathrm{e}^{\phi/\nu}. \tag{2.70}$$

The solution is completed when ϕ is determined. However, note that if $w = 0$ at some solid surface, then at that surface $\phi = \nu\ln(-A/B)$, but if $\phi =$ constant at the surface then the normal derivative $\partial\phi/\partial n \neq 0$ there, in general. This implies that the solution involves a porous surface at which suction is applied. If $\phi \to -\infty$ away from any solid boundary then $w \to A = W_0$, say. A particularly simple example has $\phi = -Vy$ and with $w = 0$ at $y = 0$ the asymptotic suction profile $w = W_0(1 - \mathrm{e}^{-Vy/\nu})$ is recovered. As an extension of this Stuart takes $\phi = -kxy$ so that with

$$u = -ky, \quad v = -kx, \quad w = W_0\left(1 - \mathrm{e}^{-kxy/\nu}\right),$$

which corresponds to uniform flow along the corner $x = 0, y \geq 0; y = 0, x \geq 0$. To sustain this flow the suction must increase linearly with distance from the corner.

Stuart also shows how this solution may be extended to the flow in a corner of any included angle less than 2π.

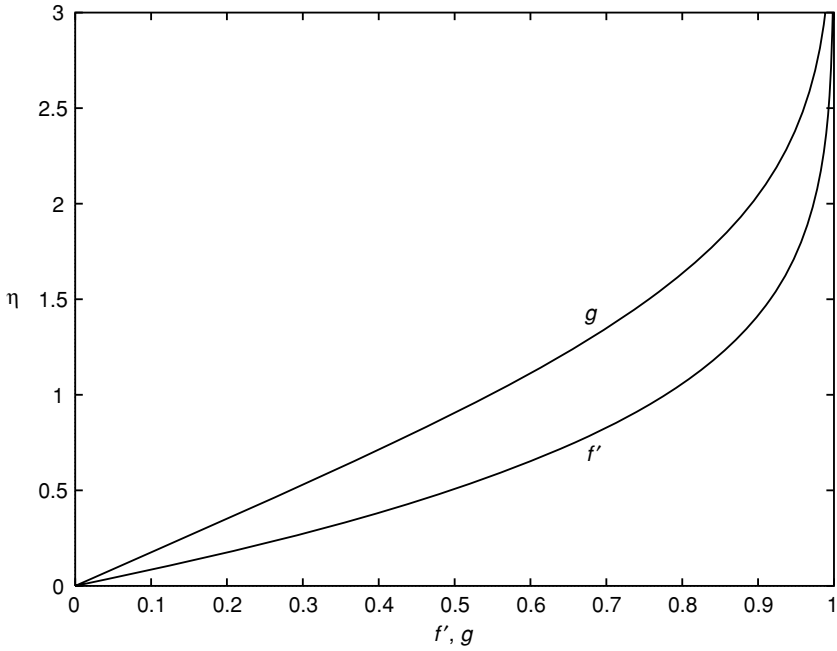

Figure 2.13 The Hiemenz velocity profile $f'(\eta)$ and the cross-flow velocity profile $g(\eta)$ at a swept stagnation line.

2.5.2 A swept stagnation flow

In section 2.3 we considered the classical stagnation-point flow appropriate, for example, to the flow at the stagnation line of a cylinder placed perpendicular to an oncoming stream. If the cylinder is 'swept', or placed at an angle to the stream, then (2.32) is supplemented by taking the third velocity component as $w = w_0 g(\eta)$ and from (1.11) and (2.32) we find

$$g'' + fg' = 0, \quad \text{with} \quad g(0) = 0, \quad g(\infty) = 1,$$

so that

$$g(\eta) = \frac{\int_0^\eta \exp\left(-\int_0^t f \, \mathrm{d}s\right) \mathrm{d}t}{\int_0^\infty \exp\left(-\int_0^t f \, \mathrm{d}s\right) \mathrm{d}t}. \tag{2.71}$$

The velocity profile $w/w_0 = g(\eta)$ is shown in figure 2.13.

Coward and Hall (1996) extend this solution to include a thin liquid film at the surface of the cylinder.

2.5.3 Vortices in a stagnation flow

Kerr and Dold (1994) have considered a flow in which, superposed upon a two-dimensional stagnation flow in the absence of any solid boundaries, is an array of counter-rotating vortices whose axes are parallel to the direction of the diverging flow. The velocity field may be written as

$$\left(\frac{A}{k}x, \quad -\frac{A}{k}y + \nu k\frac{\partial\psi}{\partial z}, \quad -\nu k\frac{\partial\psi}{\partial y}\right), \tag{2.72}$$

where A is a measure of the strength of the basic stagnation flow, $\psi = \psi(y, z)$ is a stream function made dimensionless with scale ν, and k^{-1} is a length chosen such that $2\pi/k$ is the periodic spacing in the z-direction of the vortices. The vorticity

$$\boldsymbol{\omega} = \xi\mathbf{i} = -\left(\frac{\partial^2\psi}{\partial y^2} + \frac{\partial^2\psi}{\partial z^2}\right)\mathbf{i}, \tag{2.73}$$

and the equation satisfied by the vorticity is

$$-\frac{\partial\psi}{\partial y}\frac{\partial\xi}{\partial z} + \frac{\partial\psi}{\partial z}\frac{\partial\xi}{\partial y} - \lambda y\frac{\partial\xi}{\partial y} - \lambda\xi = \frac{\partial^2\xi}{\partial y^2} + \frac{\partial^2\xi}{\partial z^2}, \tag{2.74}$$

where $\lambda = A/\nu k^2$, which may be interpreted as a measure of the strength of the converging flow to the rate of viscous diffusion.

A simple solution of the above is, for $\lambda = 1$, $\psi = \xi = \cos z$, obtained by Craik and Criminale (1986) as a special case in their examination of the stability of disturbances that consist of single Fourier modes in unbounded shear flows. For the vortex flows Kerr and Dold develop solutions of (2.73), (2.74) as

$$\xi = \sum_{n=1}^{\infty} a_n(y)\cos(2n-1)z + b_n(y)\sin 2nz,$$

$$\psi(y, z) = \sum_{n=1}^{\infty} c_n(y)\cos(2n-1)z + d_n(y)\sin 2nz.$$

Substitution into the equations for ψ, ξ yields an infinite system of ordinary differential equations, namely

$$\begin{aligned} a_n'' + \lambda y a_n' + \{\lambda - (2n-1)^2\}a_n &= F_{2n-1}(\psi, \xi), \\ b_n'' + \lambda y b_n' + (\lambda - 4n^2)b_n &= F_{2n}(\psi, \xi), \\ c_n'' + (2n-1)^2 c_n &= -a_n, \\ d_n'' - 4n^2 d_n &= -b_n, \end{aligned} \tag{2.75}$$

where F_{2n-1}, F_{2n} are the appropriate components of the non-linear terms. By symmetry we anticipate $\psi(y, z) = \psi(-y, -z) = -\psi(y, \pi - z)$ so that $a_n(y)$,

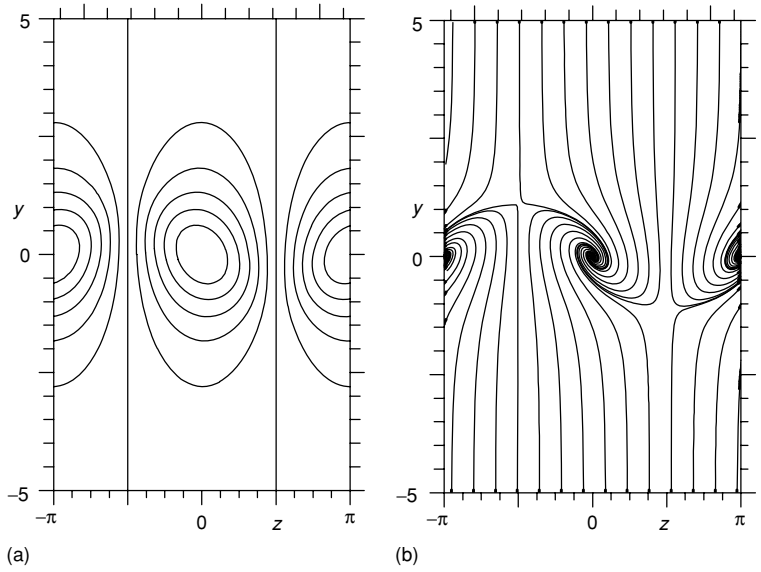

Figure 2.14 (a) Streamlines of perturbation vortices of amplitude 10 for $\lambda = 6$. (b) The corresponding streamlines for the whole flow projected onto the (y, z)-plane. (From Kerr and Dold (1994).)

$b_n(y)$ are even and odd functions of y respectively. Thus

$$a_n'(0) = b_n(0) = c_n'(0) = d_n(0) = 0,$$

and in addition we require $a_n, b_n, c_n, d_n \to 0$ as $y \to \infty$. Decay of the solutions in the far field is ensured if $\lambda > 1$; accordingly there are essentially two parameters that characterise these flows, namely λ and a second parameter that Kerr and Dold take as the amplitude of the vortices, defined as the value of the stream function at the origin. In carrying out numerical solutions of (2.75) fewer than ten terms of the series are required for a wide range of values of λ and the amplitude. An example is shown in figure 2.14.

Kerr and Dold note that the vortex structures vary only slowly as the amplitude increases from infinitesimal to large values, and that these are mirrored, to some extent, when the non-linear terms in (2.75) are ignored. That this is so may be expected, since the essential balance between diffusion of vorticity and intensification due to stretching of vortex lines is associated with the linear terms in (2.74).

Kerr and Dold note that an array of counter-rotating vortices are observed in the 'four roll mill' experiments of Lagnado and Leal (1990). The vortices appear above a critical strain rate with axes aligned with the straining flow.

Burgers (1948) and Robinson and Saffman (1984) have considered a simpler configuration, namely a shear flow in the z-direction, that nevertheless retains the essential balance between diffusion of vorticity and intensification due to stretching. Thus, with $\mathbf{v} = \{\alpha x, -\alpha y, W(y)\}$, we have $\boldsymbol{\omega} = \{\xi(y), 0, 0\}$, where $\xi = W'$ satisfies $\nu\xi'' + \alpha(y\xi)' = 0$ with solution

$$\xi = \{W(\infty) - W(-\infty)\}\left(\frac{\alpha}{2\pi\nu}\right)^{1/2}\exp(-\alpha y^2/2\nu), \tag{2.76}$$

and $W(\infty) - W(-\infty)$ is a free parameter.

2.5.4 Three-dimensional stagnation-point flow

In section 2.3 above we have considered the flow at a two-dimensional stagnation point on a plane boundary, and in the next chapter we shall discuss its axisymmetric analogue. Both of these are special cases of a three-dimensional stagnation-point flow on a plane boundary, first considered by Howarth (1951). For consistency with the established literature, and with chapter 3, we adopt a slight change of notation so that x, y are co-ordinates in the plane, with z perpendicular to it. With $u = kx$, $v = ly$ at large distances from the boundary it proves convenient to write

$$u = kxf'(\eta), \quad v = kyg'(\eta), \quad w = -(\nu k)^{1/2}\{f(\eta) + g(\eta)\}, \quad \eta = \left(\frac{k}{\nu}\right)^{1/2} z, \tag{2.77}$$

so that, with $r = l/k$, substitution into equations (1.9) to (1.11) gives, as equations for f and g,

$$f''' + (f+g)f'' + 1 - f'^2 = 0, \quad g''' + (f+g)g'' + r^2 - g'^2 = 0,$$

with the pressure determined as

$$\frac{p_0 - p}{\rho} = \frac{1}{2}(k^2x^2 + l^2y^2) + \nu k(f' + g') + \frac{1}{2}\nu k(f+g)^2.$$

The boundary conditions require

$$f(0) = g(0) = f'(0) = g'(0) = 0, \quad f'(\infty) = 1, \quad g'(\infty) = r.$$

Howarth obtained solutions for f and g for a range of values of r with $0 \le r \le 1$. These solutions correspond to the flow in the immediate neighbourhood of a nodal point of attachment as might be found, for example, at an asymmetric protuberance on a body placed in a uniform stream parallel to the z-direction. Subsequently Davey (1961) obtained solutions for a range of negative values of r with $-1 \le r < 0$. Such solutions correspond to a saddle point of

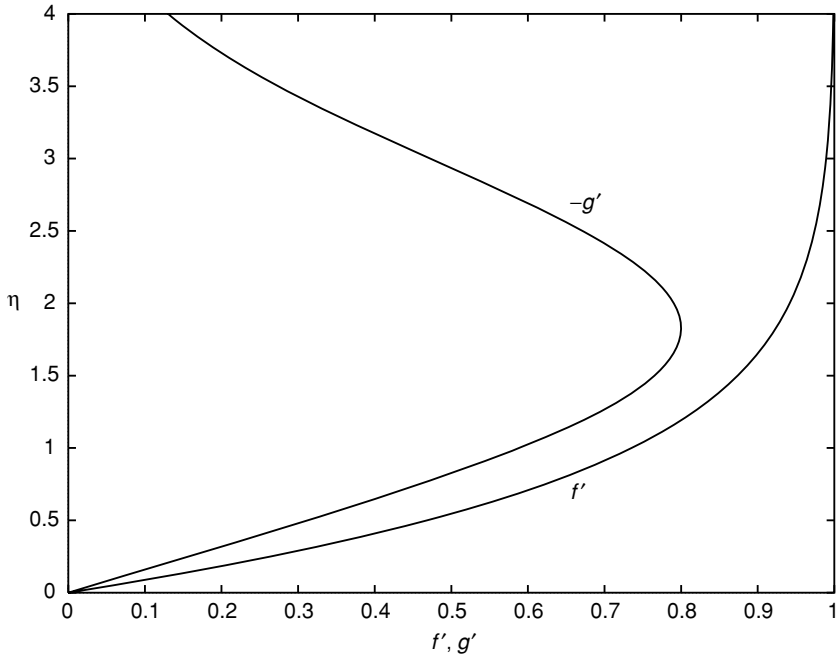

Figure 2.15 Velocity profiles for the dual of the two-dimensional stagnation-point flow (i.e. $r = 0$) obtained by Davey and Schofield (1967).

attachment which may be found, for example, in the immediate neighbourhood of a geometrical saddle point on the surface of a body located between two protuberances. From a topological viewpoint Davey establishes that on a finite body the number of nodal points must exceed the number of saddle points by two. He also proves that for $r < -1$ which, as we see from (2.77), corresponds to a saddle point of separation, the equations have no solution.

Subsequently Libby (1967), Davey and Schofield (1967) and Schofield and Davey (1967) revisited the problem and demonstrated the existence of dual solutions of (2.77). Libby suggested non-uniqueness for $r < 0$ and gave some examples. Schofield and Davey, however, demonstrated the existence of a dual for each of the solutions obtained by Howarth (1951) and Davey (1961) in the range $-1 \leq r \leq 1$. The particular case $r = 0$ was discussed in detail by Davey and Schofield. This corresponds to a three-dimensional solution of the Navier–Stokes equations embedded in what is essentially a two-dimensional stagnation point of attachment. Solutions were obtained numerically by Davey and Schofield and we show the velocity profiles $f'(\eta)$, $g'(\eta)$ in figure 2.15. Similarly, when $r = 1$, the dual of the axisymmetric problem is asymmetric.

Some years later Hewitt, Duck and Stow (2002) showed that these two solution branches, for which $1 - f', r - g'$ are exponentially small as $\eta \to \infty$, are just the first two of a countably infinite sequence of such states.

Libby (1974) has extended the analysis of Rott (1956) for a two-dimensional stagnation point at a sliding boundary to the three-dimensional case. Thus, the velocity components u, v in equation (2.77) are replaced by

$$u = u_w F(\eta) + kxf'(\eta), \quad v = v_w G(\eta) + lyg'(\eta),$$

and the ordinary differential equations satisfied by F and G integrated numerically. The constants u_w, v_w represent the velocity of the boundary. This solution finds application, for example, to the flow at a stagnation point on an ellipsoid rotating about one of its axes.